

Bright aspects of defect and dark traits of dopant in photoluminescence of $\text{Er}_2\text{X}_2\text{O}_7:\text{Eu}^{3+}$ (X=Ti and Zr) pyrochlore: An insight using EXAFS, Positron and DFT

Santosh K. Gupta^{1*}, K. Sudarshan^{1,6}, Paramananda Jena,² P.S. Ghosh³, A.K. Yadav⁴, S.N. Jha^{5,6}, D. Bhattacharyya^{4,6}

¹Radiochemistry Division, Bhabha Atomic Research Centre, Trombay, Mumbai-400085, India

²School of Materials Science & Technology, Indian Institute of Technology (Banaras Hindu University), Varanasi-221005, Uttar Pradesh, India

³Glass and Advanced Materials Division, Bhabha Atomic Research Centre, Trombay, Mumbai-400085, India

⁴Atomic and Molecular Physics Division, Bhabha Atomic Research Centre, Trombay, Mumbai-400085, India

⁵Beamline Development & Application Section, Bhabha Atomic Research Centre, Trombay, Mumbai-400085, India

⁶Homi Bhabha National Institute, Anushaktinagar, Mumbai – 400094, India

*To whom correspondence should be addressed. Electronic mail: santoshg@barc.gov.in, santufrnd@gmail.com, Tel.: +91-22-25590636

S1. Synthesis:

$\text{Er}_2\text{Zr}_2\text{O}_7$ (EZO) and $\text{Er}_2\text{Ti}_2\text{O}_7$ (ETO) samples were synthesized by using a simple, scalable and industrially viable high energy ball milling (RETSCH-PM 400, Gmbh, Germany) method. Analar grade precursor chemicals such as Erbium oxide [Er_2O_3 , Sigma-Aldrich 99.90%], Zirconium dioxide [ZrO_2 , Hi-media, 99.00%], Titanium dioxide [TiO_2 , Hi-media, 99.00%], and absolute ethanol (Loba) as a solvent were used for the synthesis. The chemicals were used as received without further purification. The required stoichiometric amount of precursor chemicals such as Erbium oxide (Er_2O_3), Zirconium dioxide (ZrO_2), Titanium dioxide (TiO_2) were weighed separately and then mixed each other. Further the mixtures were transferred to a grinding jar made of zirconia. The ethanol was used as milling medium. The zirconia balls were used as grinding medium. The ball to powder ratios was kept at 10:1. The milling speed was set at 300 rpm for 16 hr with an interruption of 60 seconds clock wise and 60 seconds anti clock wise. The prepared product was collected from grinding jar and subsequently dried at 60 °C for 12 h on hot plate. The obtained dried sample is calcined at 800 °C for 6 hours and 1500 °C for 6 hours with grinding the sample in between two calcination steps. For the preparation of Eu^{3+} doped samples of $\text{Er}_2\text{Zr}_2\text{O}_7$ (EEZO) and $\text{Er}_2\text{Ti}_2\text{O}_7$ (EETO), Eu_2O_3 was added to the mixture before milling and calcination.

S2. Characterization

Powder X-ray diffraction measurements were carried in the 2θ angle range of 10-80° with diffractometer, RigakuMiniflex/600, using Cu K_α radiation. Rietveld refinement was carried out using FULLPROF suit [1] with sixth order polynomial background and Pseudo-Voigt functions

for profile analysis. Photoluminescence measurements were carried out using Edinburgh CD-920 spectrometer coupled to F-900 software. Positron lifetime spectra were measured using a lifetime spectrometer having a time resolution of 265 ps and PALSFit software [2] was used for the analysis of the spectra.

EXAFS measurements are done on ETO and EZO to probe the local structure surrounding the Er, Zr and Ti sites. The EXAFS measurements have been carried out at the Energy-Scanning EXAFS beamline (BL-9) at the INDUS-2 Synchrotron Source (2.5 GeV, 100 mA) at Raja Ramanna Centre for Advanced Technology (RRCAT), Indore, India. This beamline operates in energy range of 4 KeV to 25 KeV. The beamline optics consist of a Rh/Pt coated collimating meridional cylindrical mirror and the collimated beam reflected by the mirror is monochromatized by a Si(111) (2d=6.2709) based double crystal monochromator. The second crystal of DCM is a sagittal cylinder used for horizontal focusing while a Rh/Pt coated bendable post mirror facing down is used for vertical focusing of the beam at the sample position. Rejection of the higher harmonics content in the X-ray beam is performed by detuning the second crystal of DCM. In the present case, EXAFS measurements have been performed in transmission mode.

For the transmission measurement, three ionization chambers (300 mm length each) have been used for data collection, one ionization chamber for measuring incident flux (I_0), second one for measuring transmitted flux (I_t) and the third ionization chamber for measuring EXAFS spectrum of a reference metal foil for energy calibration. Appropriate gas pressure and gas mixtures have been chosen to achieve 10-20% absorption in first ionization chamber and 70-90% absorption in second ionization chamber to improve the signal to noise ratio. The absorption coefficient μ is obtained using the relation:

$$I_t = I_0 e^{-\mu x} \quad (1)$$

where, x is the thickness of the absorber.

In order to take care of the oscillations in the absorption spectra $\mu(E)$ has been converted to absorption function $\chi(E)$ defined as follows:[3]

$$\chi(E) = \frac{\mu(E) - \mu_0(E)}{\Delta\mu_0(E_0)} \quad (2)$$

Where, E_0 is absorption edge energy, $\mu_0(E_0)$ is the bare atom background and $\Delta\mu_0(E_0)$ is the step in $\mu(E)$ value at the absorption edge. The energy dependent absorption coefficient $\chi(E)$ has been converted to the wave number dependent absorption coefficient $\chi(k)$ using the relation,

$$K = \sqrt{\frac{2m(E - E_0)}{h^2}} \quad (3)$$

where, m is the electron mass. $\chi(k)$ is weighted by k^2 to amplify the oscillation at high k and the $\chi(k)k^2$ functions are Fourier transformed in R space to generate the $\chi(R)$ versus R spectra in terms of the real distances from the center of the absorbing atom. The set of EXAFS data analysis programme available within Demeter software package have been used for EXAFS data analysis.[4] This includes background reduction and Fourier transform to derive the $\chi(R)$ versus R spectra from the absorption spectra (using ATHENA software), generation of the theoretical EXAFS spectra starting from an assumed crystallographic structure and finally fitting of experimental data with the theoretical spectra using ARTEMIS software.

S3. Theoretical Methodology:

All the electronic structure calculations of ordered pyrochlore ($\text{Er}_2\text{Ti}_2\text{O}_7$, ETO) and disordered fluorite ($\text{Er}_2\text{Zr}_2\text{O}_7$, EZO) structures were performed using a plane wave based spin-polarized density functional theory (DFT) as implemented in Vienna Ab-initio Simulation package (VASP) [5,6]. The electron-ion interaction was described by projector augmented wave (PAW) potential [7] which includes the valence states of Er₃ ($5s^2 6s^2 5p^6 6d^1$ - 9 valence electrons), Ti ($3s^2 3p^6 4s^2 3d^2$ -12 valence electrons), Zr ($4s^2 4p^6 5s^2 4d^2$ - 12 valence electrons) and O ($2s^2 2p^4$ - 6 valence electrons). The generalized gradient approximation (GGA) with Perdew-Burke-Ernzerhof (PBE) parameterization [8] was used for the exchange-correlation part. A Monkhorst-Pack [9] k -space mesh of $4 \times 4 \times 4$ in reciprocal space for the Brillouin zone integration was used for the 88 atoms cells. The plane wave cutoff energy (E_{cut}) of 600 eV for basis set was used throughout the simulation. The optimization was carried out to get converged values for E_{cut} and k -point meshes which ensure convergence of total energy to within a precision 0.05 meV/atom. The cohesive energy of ETO and EZO were optimized with respect to volume (or lattice parameter) and atomic positions using conjugate gradient algorithm until the residual forces and stress in the equilibrium geometry were of the order of 0.005 eV/Å and

0.01GPa, respectively. The final calculation of total electronic energy and density of states (DOS) were performed using the tetrahedron method with Blöchl corrections [10].

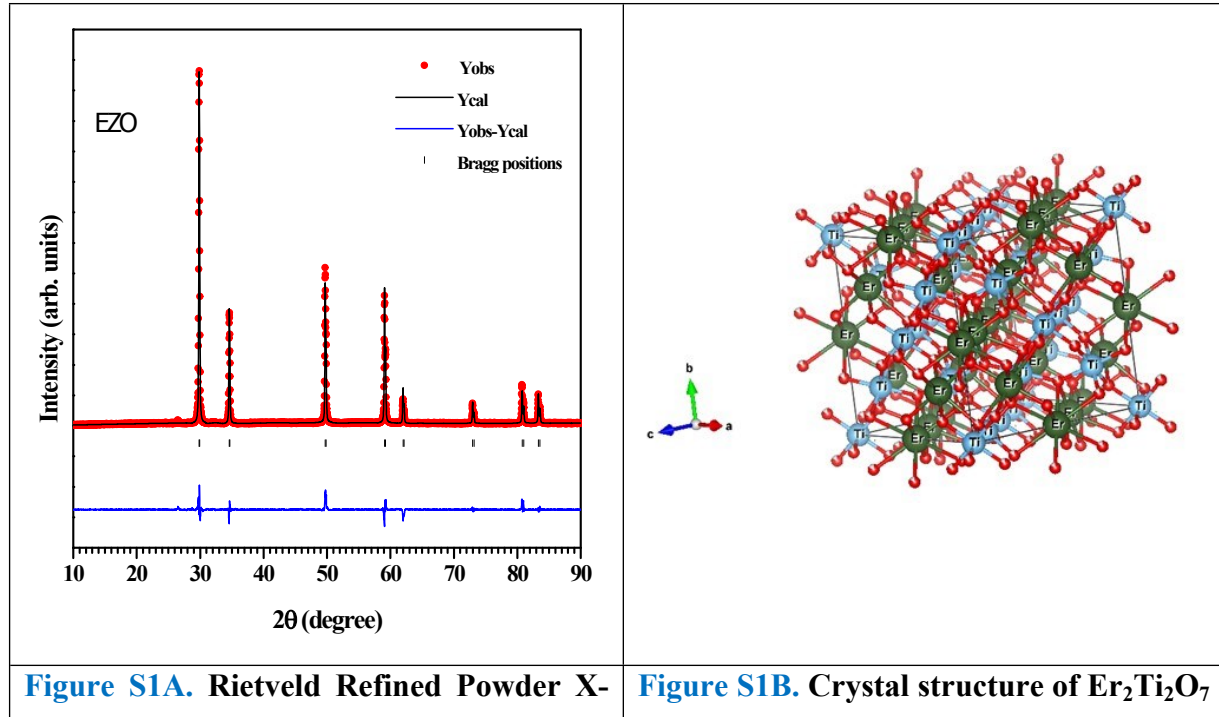
All the calculations were performed on a 88 atom supercell for both ordered pyrochlore and disordered fluorite. For ordered pyrochlore 88-atom supercell is a standard 2x2x2 cell of 22 atom primitive cell and an 88-atom Special Quasi-random Structure (SQS) for the fully disordered $(A_{1/2}B_{1/2})(O_{7/8}V_{1/8})_2$ defect-fluorite structure was used. This structure was generated using Monte-Carlo simulated annealing technique [11].

The defect formation energy is given by

$$E_f^q = E_{defect}^q - E_{perfect} - \sum_{\alpha} n_{\alpha} \mu_{\alpha} + q_i \mu_e + dE$$

where E_{defect}^q and $E_{perfect}$ are the DFT(GGA) total energies of the system with and without the defect respectively, n_{α} is the number of atoms added/removed, μ_{α} is the chemical potential of the species α that is added/removed, q_i is the effective charge on the defect and $\mu_e = E_{VBM} + \epsilon_F$. E_{VBM} is the energy of the valence band maximum (VBM) and ϵ_F is the electron chemical potential above the VBM. dE is a correction used to mitigate the interactions of the defect charges with their periodic images. Here we employ a Madelung correction as proposed by Leslie and Gillan [12]

S4. Rietveld refined XRD pattern:



ray diffraction pattern of $\text{Er}_2\text{Ti}_2\text{O}_7$	with Fd-3m space group
---	---------------------------------

Table S1: Refined structural parameters obtained from the Rietveld analysis of the $\text{Er}_2\text{Ti}_2\text{O}_7$ sample

Structural parameters	Obtained values
$a = b = c$ (Å)	10.0934 (2)
Unit cell volume(Å ³)	1028.297
R_p	10.2
R_{wp}	14.1
R_{exp}	8.88
Chi^2 (χ^2)	2.52

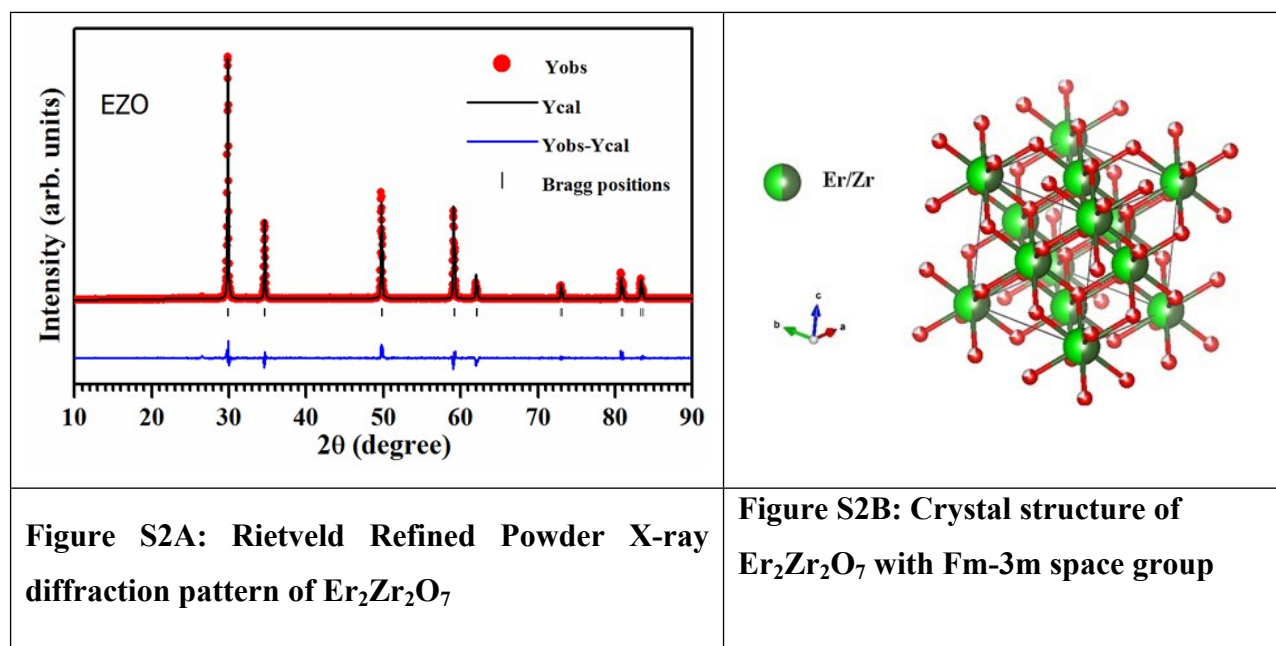


Table S2. Refined structural parameters obtained from the Rietveld analysis of the $\text{Er}_2\text{Zr}_2\text{O}_7$ sample

Structural parameters	Obtained values
-----------------------	-----------------

a = b = c (Å)	5.1822 (1)
Unit cell volume(Å ³)	139.17
S.G.	Fm-3m
R _p	8.03
R _{wp}	10.7
R _{exp}	7.78
Chi ² (χ ²)	1.88

References:

1. J. Rodríguez-Carvajal, Introduction to the program FULLPROF: refinement of crystal and magnetic structures from powder and single crystal data, Laboratoire Léon Brillouin (CEA-CNRS): Saclay, France (2001)
2. P. Kirkegaard, J.V. Olsen, M. Eldrup, N.J. Pedersen, PALSfit: A computer program for analysing positron lifetime spectra, Risø National Laboratory for Sustainable Energy, Technical University of Denmark, Roskilde, Denmark, Risø (2009).
3. D. Konigsberger, R. Prins, X-ray absorption: principles, applications, techniques of EXAFS, SEXAFS and XANES, Wiley/Interscience, New York 159 (1988) 160.
4. M. Newville, B. Ravel, D. Haskel, J. Rehr, E. Stern, Y. Yacoby, Analysis of multiple-scattering XAFS data using theoretical standards, PHYSICA B 208 (1995) 154-154
5. G. Kresse and J. Furthmueller, Phys. Rev. B: Condens. Matter Mater. Phys. 5 (1996) 11169.
6. G. Kresse and J. Furthmueller, Comput. Mater. Sci. 6 (1996) 15.
7. P. E. Blochl, Phys. Rev. B: Condens. Matter Mater. Phys. 50 (1994) 17953.
8. J. P. Perdew, K. Burke and M. Ernzerhof, Phys. Rev. Lett. 77 (1996) 3685.
9. H. J. Monkhorst and J. D. Pack, Phys. Rev. B: Condens. Matter Mater. Phys. 13 (1979) 5188.
10. P. E. Blochl, O. Jepsen and O. K. Andersen, Phys. Rev. B: Condens. Matter Mater. Phys. 4 (1994) 16223.
11. Chao Jiang, C. R. Stanek, K. E. Sickafus, and B. P. Uberuaga, Phys. Rev. B 79 (2009) 104203.

12. M. Leslie, M.J. Gillan, J. Phys. C 18 (1985) 973-982.